Estimating Bulk Geometrical Properties of Cellular Structures

Shannon Puddister*, David A. Clausi*, G. Wayne Brodland
*Department of Systems Design Engineering (519-888-4567 x2604)
**Department of Civil Engineering (519-888-4567 x6211)
University of Waterloo, Waterloo, ON, Canada, N2L 3G1
{smpuddis,dclausi,brodland}@uwaterloo.ca

Abstract

Three algorithms for determining the bulk geometric properties of cellular structures from a stationary digital image are presented. The geometrical properties of interest include cell orientation and cell aspect ratio. With future test data expected to possess high luminance variability, poor contrast near element boundaries and irregular discolouration, this problem is poorly suited for the spatial techniques currently in the computer vision literature. Algorithms operating within the spatial-frequency domain based on Gabor filters, area moments (moments of inertia) and least squares ellipse fitting are used to determine the bulk geometrical properties of cellular structures in a digital image.

Keywords: geometrical parameter estimation, Gabor filters, area moments, least squares, spatial-frequency, biological cells

1. INTRODUCTION

Automatically extracting meaningful bulk shape and orientation information from a stationary digital image is a difficult task for a computer algorithm. For example, cells arranged in a planar sheet that are imaged using a high resolution camera will tend to have similar aspect ratios and orientations. Unfortunately, due to camera limitations (eg. resolution and lighting) and environmental issues (eg. pigmentation variation and cell division), automated quantitative geometrical interpretation is not straightforward. Developing a quantitative understanding of the geometrical properties of embryonic cells provides key information for understanding the biomechanical basis of embryonic development [4]. Another example of consistent geometrical characteristics in imagery is the estimation of ice floe size in synthetic aperture radar (SAR) sea ice images. Ice fields often generate consistent ice floe sizes and it is desirable, from an operational perspective, to understand the geometrical characteristics of the floes in a particular ice field. Again sensor limitations (eg. speckle noise) and environmental conditions (eg. local weather) prevent the use of spatial techniques to generate bulk geometrical estimates [3]. Each object in such imagery has its own geometrical properties which are similar to its neighbours. As a result, there are bulk geometrical properties that can be used to describe the general characteristics of the objects in the image. The objective of this research is to generate automated methods to produce such estimates.

Spatial domain techniques (eg. edge detection, snake contours, watershed algorithms) are extremely sensitive to local noise processes. Many of the natural boundaries are not clearly visible. Standard computer algorithms are not able to handle such variability and are not sufficiently effective in dealing with natural imagery. In order to estimate the bulk geometric characteristics on a global basis, the spatial-frequency domain representation of the image is considered. To the best knowledge of the authors, such an approach is novel. This transformation can provide the information necessary to estimate the geometrical parameters of interest. The power spectrum will be distributed somewhat elliptically, a result of the assumptions of consistent shape and orientation in the presence of noise in the image under consideration.

Using the spatial-frequency domain, there are two primary spatial geometrical parameters that will be estimated: (1) the aspect ratio (the ratio of the element length to width) and (2) the orientation of elements as measured counter-clockwise from the horizontal ($-\pi/2<\theta<\pi/2$). A number of different techniques can be used to extract meaningful information from the spatial-frequency representation. Gabor filters, effectively band pass filters, can be tuned to generate an optimal response which in turn reflects the dominant frequency components in the image. By estimating area moments in the spatial-frequency domain, both the aspect ratio and orientation can be determined. Finally, an elliptical least squares approach can be used to estimate the observed elliptical shape in the power spectrum.

This paper proceeds in the following fashion. Sample images with known geometrical parameters are presented. A variety of techniques that can be used to estimate geometrical properties are described. These techniques include Gabor filters, area moment estimation, and least squares elliptical fitting. Testing of each image with respect to each technique follows. The paper finishes with conclusions and future directions.

2. METHODS

2.1 Data

Figures 1(a) and 1(b) depict test images used for the algorithm development. Figure 1(a) is Brodatz image D95 (Brick) [2], rotated by 47.5 degrees counter-clockwise from the horizontal. The second image, Figure 1(b), is a synthetic mesh representing the cells in an epithelium made by annealing a Voronoi tessellation, which was then stretched by a factor of two and rotated by 30 degrees counter-clockwise from the horizontal [4].

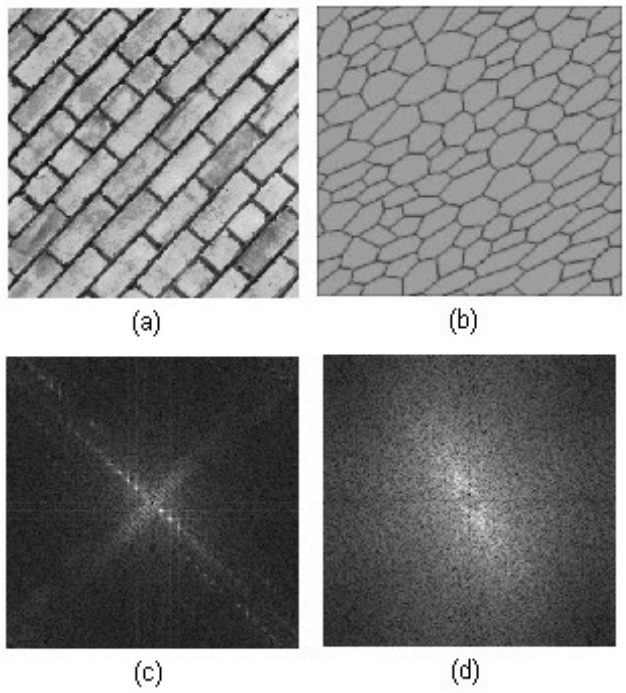

Figure 1 (a) Brodatz Brick (D95), (b) Synthetic mesh representing cells in an epithelium, (c) Power spectrum of Figure 1(a), (d) Power spectrum of Figure 1(b).

Figure 1(c) and 1(d) are the FFT spatial-frequency magnitude representations of the brick and synthetic cell images, respectively. To enhance the visual image content, the square root operator is applied after the DC component is removed. The algorithms described in this paper function by isolating features in the power spectrum that correspond with the required spatial geometric properties.

As a descriptive example of these geometric properties, visual inspection of Figure 1(a) indicates that, on average, individual bricks are rotated by approximately 45 degrees and have an aspect ratio of approximately 2:1. In each method presented, the orientation is first computed. Metrics to describe the length and width of the object that best characterizes the spatial image are then obtained. Measured in the power spectrum, the length and the width are expressed in units of cycles per image. The dominant orientation of the power spectrum, that is, the angle at which the data appears stretched and furthest from the image centre (ie. at highest frequencies) corresponds to the image object width. This should be intuitive, since the width, the shorter of the two length metrics, would have more cycles across an image.

2.2 Gabor Filter Optimization

The Gabor function is a band-pass filter. Its 2-d representation is able to estimate the energy of a signal given a specified frequency and orientation. Its representation in the spatial-frequency domain is tractable since it is simply a Gaussian centered at the frequency of interest. These capabilities have motivated the successful application of Gabor filter banks in a pseudo-wavelet framework for image texture segmentation [5][7].

Gabor filters can also be used to extract the bulk geometrical properties in images such as those found in Figure 1. The Gabor filter that generates the maximum response of all possible configurations is deemed to identify the dominant orientation and frequency in the image. Since an exhaustive selection of the Gabor filter parameters is unrealistic (there are four real-valued parameters to set), an optimization framework was implemented. Here, the method described by Torczon [12] was utilized.

While this approach generated accurate geometrical values on "clean" images such as the brick image of Figure 1(a), it was only able to consistently determine the frequency-orientation pair along the dominant axis in the synthetic cell data in Figure 1(b), and not the frequency along the perpendicular axis, as required. Since it is desired to create a robust and generic algorithm capable of operating in the presence of considerable noise, Gabor filtering was not considered further and, for succinctness, results will not be reported.

2.3 Moments of Inertia

The area moments provide information about the geometric characteristics of an object about a fixed point. Calculating the area moments, I_{xx} and I_{yy}, and the product of inertia, I_{xy}, in the power spectrum provides a means of estimating the desired aspect ratio and orientation of the objects in the spatial domain. These inertial measures are determined as follows:

$$I_{xx} = \sum_{y=1}^{rows}\sum_{x=1}^{cols} F(x,y)\cdot y^2$$

$$I_{yy} = \sum_{y=1}^{rows}\sum_{x=1}^{cols} F(x,y)\cdot x^2$$

$$I_{xy} = \sum_{y=1}^{rows}\sum_{x=1}^{cols} F(x,y)\cdot x\cdot y$$

where x is the column index, y is the row index, *rows* is the number of rows, *cols* is the numbers of columns, and F is the image's power spectrum [9]. After computing these values, the dominant orientation is calculated as:

$$\theta = \arctan\left(\frac{2I_{xy}}{I_{xx}-I_{yy}}\right), \text{ provided } I_{xx} \neq I_{yy}.$$

In the case that $I_{xx} = I_{yy}$,

$$\theta = \begin{cases} \pi/4 & , \quad I_{xy} > 0 \\ 0 & , \quad I_{xy} = 0 \\ -\pi/4 & , \quad I_{xy} < 0 \end{cases}.$$

Moment-based computations can also directly determine the aspect ratio of the ellipse in the power spectrum. However, the noise in the power spectrum of a natural image renders such a direct approach infeasible and an alternative method was required.

A statistical method based on the computed orientation was used to extract the frequency values required to calculate the aspect ratio. This was done by projecting all points within a narrow three pixel band of the major and minor axes onto a line. This narrow band was chosen so as to minimize the effects of high frequency noise while maximizing the contribution of local pixels. Subpixel calculations are made by weighing the contribution of neighbouring pixels proportionate to their subpixel distance along the projection. Gaussian smoothing ($\sigma = 1$ pixel) was applied to the projected data and the coordinate associated with the maximum value was determined. This value is considered to be the frequency most representative of the image along the projected orientation. Along the dominant axis, this frequency is considered the average width, and along the axis perpendicular to the dominant axis, the average length of objects in the spatial domain.

2.4 Least Squares Ellipse Fitting

Least squares methods are commonly used to estimate the necessary parameters for a straight line given appropriate data. Here, an elliptical least squares approach is used to estimate the parameters of an ellipse given elliptically-distributed data, such as that observed in Figure 1(d).

Numerous methods have been developed for fitting ellipses to data points, each with varying levels of success. Many of these techniques [1][10][11] attempt to fit data points to a general conic and rely on an additional constraint to force the solution to an ellipse. In [6], Fitzgibbon presented a direct least squares based ellipse specific method, and contrasted this method to earlier ones. In this method, the general conic is represented by the second order polynomial:

$$G(\boldsymbol{r}, \boldsymbol{x}) = \boldsymbol{r}\cdot\boldsymbol{x} = ax^2 + bxy + cy^2 + dx + ey + f = 0,$$

where

$$\boldsymbol{r} = [\, a \;\; b \;\; c \;\; d \;\; e \;\; f \,]^T$$

$$\boldsymbol{x} = [\, x^2 \;\; xy \;\; y^2 \;\; x \;\; y \;\; 1 \,]^T$$

and with an ellipse-specific constraint

$$b^2 - 4ac < 0\,.$$

Fitting a general conic to the data was then a matter of minimizing the sum of the squared algebraic distances of the curve to the data points x_i.

$$D_A(r) = \sum_{i=1}^{n} F(x_i)^2\,.$$

A computationally inexpensive algorithm results. Furthermore, since it was specifically designed for fitting data to an ellipse, the algorithm is robust in the presence of noise. Improvements based on the MATLAB code that implemented the algorithm presented by Fitzgibbon were made by Pilu [8]. This code, which enhanced the numerical stability of the computation and presented the output in a manner more suitable to this application, was used for the implementation of this algorithm. The output from this least squares algorithm is the ellipse orientation,

as well as the lengths of the major and minor axes which were used to compute the aspect ratio.

3. EXPERIMENT AND RESULTS

In this section, the methods described in Sections 2.3 and 2.4 are applied to the data shown in Figure 1(c) and 1(d). The method of determining the bulk statistics using area moment measurements is presented first. In Figure 2, the spatial frequency representations of the original data are shown with the computed orientation axes superimposed. It is on these lines that the neighbouring pixels will be projected in order to statistically determine the frequencies. The bulk statistics, as produced by the moment-based and the least squares ellipse fitting algorithm are shown in Table 1.

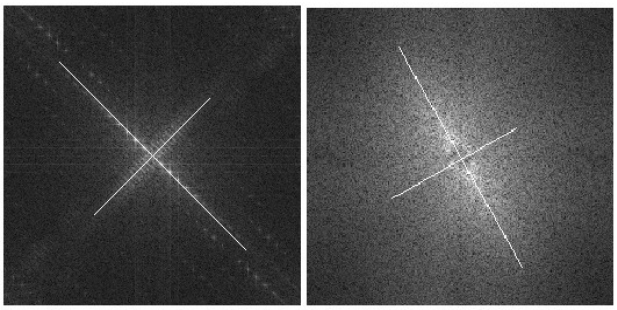

Figure 2 The power spectrums of the brick (left) and synthetic cell (right) data is shown above with major and minor axes superimposed, as determined by the area moment-based algorithm.

Table 1 Actual and computed values for the bulk statistics in brick and synthetic cell data as generated by the area moments (AM) and least squares ellipse fitting (LSEF) algorithms.

Methods		Orientation (degrees)	Aspect Ratio (κ)
Brick Data	Actual	47.5	2.0
	AM	46.5	1.8
	LSEF	47.5	2.0
Synthetic Cell Data	Actual	~30	~2.0
	AM	29.5	1.7
	LSEF	32.8	2.7

It is observed that the orientations as computed by the moment-based algorithm are very close to the actual values. In the case of the brick data, the rotation was off by one degree. The synthetic data was measured to within half a degree of the actual value. With regards to frequencies, this algorithm produced results that might be expected from visual inspection of the data.

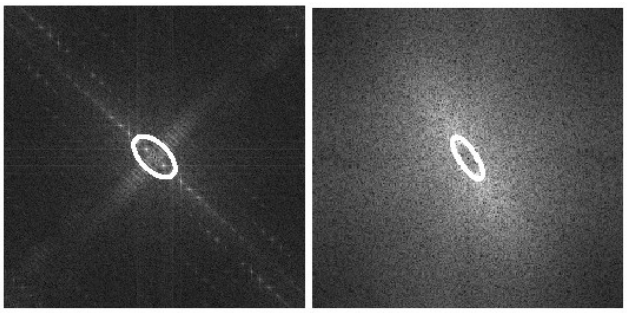

Figure 3 The power spectrums of the brick (left) and synthetic cell (right) data is shown above with an ellipse fitted to the data, as determined by the least squares ellipse fitting algorithm.

The least squares ellipse algorithm was implemented such that a threshold value was used below which pixels would not be considered if their associated intensities were not sufficiently high. Images whose power spectrums were concentrated about a few points would perform well without thresholding, while those that were well dispersed experienced improved performance with a high threshold. In the examples provided in Figure 3, the power spectrums were scaled so that intensities of each pixel fell between zero and one. In the case of the brick image, the best measure was obtained when the threshold was set to zero and all pixels contributed to the final ellipse. With the synthetic cell data, however, a well-fitting ellipse was obtained when the threshold was set so that only pixels with greater than 70% of the maximum intensity were considered. The reason for this discrepancy in threshold value is simply that with well-dispersed power spectrums, the data the ellipses are fit to consistently contain more energy outside the *ideal* ellipse than inside. Fortunately, similar images have similar power spectrums, so data specific bulk statistics estimation applications could be designed with tailored threshold values. Methods for automatically determining optimal threshold values could be further investigated.

Comparing the data in Table 1, the results generated by the algorithms are promising, particularly for the moment-based method. The least square ellipse fitting algorithm was able to accurately determine the orientation of the elements of an image, but fitting an ellipse to the data so that the frequencies matched the major and minor axes in the presence of considerable noise proved

challenging.

4. CONCLUSIONS

Three algorithms have been developed and implemented to estimate the bulk geometric properties of cellular structures in digital imagery. The geometric properties of interest included the aspect ratio and orientation. Gabor filters were deemed unsuitable for this application, given natural imagery. Both moments and ellipse least squares fitting generated appropriate results for the test data.

Overall, the results indicate that there is merit in approaching the quantifying of bulk geometric statistics from a global perspective. Whereas measuring by hand the localized cellular elements in an attempt to create statistical generalizations is time consuming and automated methods based on local information are not suitable for the images being considered, spatial-frequency domain techniques generated promising results. A more detailed examination will continue as spatial-frequency techniques are applied to more poorly defined natural data, such as images of cells in an epithelium and sea ice floes in SAR imagery.

REFERENCES

[1] F.L. Bookstein. Fitting conic sections to scattered data. *Computer Graphics and Image Processing,* 9, 1979, 56-71.

[2] P. Brodatz. *Textures: A Photographic Album for Artists and Designers*. Dover, New York, 1966.

[3] F. Carsey. Review and status of remote sensing of sea ice. *IEEE Journal of Oceanic Engineering*, 14 (2), 1989, 127-138.

[4] H.H. Chen, G.W. Brodland. Cell-level finite element studies of viscous cells in planar aggregates. *ASME Journal of Biomechanical Engineering*, 122, 2000, 394-401.

[5] D.A. Clausi, M.E. Jernigan. Designing Gabor filters for optimal texture separability. *Pattern Recognition*, 33, 2000, 1835-1849.

[6] A. Fitzgibbon, M. Pilu, R.B. Fisher. Direct Least Square Fitting of Ellipses. *Pattern Analysis and Machine Intelligence*, 21 (5), 1999, 476-480.

[7] A.K. Jain, F. Farrokhnia. Unsupervised texture segmentation using Gabor filters. *Pattern Recognition*, 24 (12), 1991, 1167-1186.

[8] M. Pilu. Set of MATLAB files for ellipse fitting. Hewlett-Packard Laboratories, *http://www-uk.hpl.hp.com/people/mp/research/ellipse.htm,* 1999

[9] E.P. Popov. *Mechanics of Materials*. Prentice-Hall, New Jersey, 1976

[10] P.D. Sampson. Fitting conic sections to very scattered data: An iterative refinement of the Bookstein algorithm. *Computer Graphics and Image Processing*, 18, 1982, 97-108.

[11] G. Taubin. Estimation of planar curves, surfaces and non planar space curves defined by implicit equations, with applications to edge and range image segmentation. *IEEE Trans. Pattern Analysis and Machine Intelligence*, 13 (11), 1991, 1115-1138.

[12] V. Torczon. On the convergence of pattern search algorithms. *SIAM Journal of Optimization*, 7 (1), 1997, 1-25.